

High permittivity regions in Oceanus Procellarum and Mare Imbrium found by SELENE (Kaguya)

KUMAMOTO, Atsushi^{1*}; ISHIYAMA, Ken¹; OSHIGAMI, Shoko²; HARUYAMA, Junichi³; GOTO, Yoshitaka⁴

¹Tohoku University, ²National Astronomical Observatory of Japan, ³JAXA/ISAS, ⁴Kanazawa University

Introduction: The effective permittivity of the lunar surface material is important for discussion of their composition and porosity. Based on the Maxwell-Garnett mixing model, the bulk density of the lunar surface materials can be derived from their effective permittivity by using the following equation [Fa and Wieczorek, 2012]: $\rho [\text{g/m}^3] = 4.61 (\epsilon_r - 1) / (\epsilon_r + 2)$. Bulk density of the lunar surface material depends on the abundances of voids and heavy components such as ilmenite. The dataset obtained by Lunar Radar Sounder (LRS) onboard SELENE (Kaguya) [Ono et al., 2010] enables us to perform global high-resolution mapping of the lunar surface permittivity because the observation was performed from the polar orbiter at an altitude of about 100 km, and in a frequency range around 5 MHz where thermal emissions is negligible. We should note that the echo powers from the lunar surface depends not only on the permittivity but also on the roughness of the lunar surface. As for the roughness, we can use SELENE Digital Terrain Model (DTM) based on Terrain Camera (TC) observation [Haruyama et al., 2008]. We can therefore calculate expected echo powers by applying Kirchhoff Approximation (KA), and compare them with observed echo powers in order to determine the effective permittivity.

Analyses Method: The global distributions of the intensity of the off-nadir surface echo in a frequency range of 4 - 6 MHz in an incident angle range from 10 to 20 degrees were derived from the SELENE/LRS dataset. The median of off-nadir echo intensities were derived in 360 x 180 areas of 1 degree (longitude) x 1 degree (latitude). In addition, we have derived the global distribution of the surface roughness parameters. The RMS height ν can be derived from the SELENE TC/DTM. If we assume the self-affine surface model, the roughness parameters H and s can be obtained by the least square fitting: $\nu = s \Delta x^H$ in a baseline length Δx range from 30 m to 3 km. The off-nadir surface echo power was then calculated by using the radar equation. Assuming KA, the backscattering coefficient in the radar equation can be obtained from the roughness parameters H , s [Bruzzone et al., 2011]. In calculation of the expected echo powers, we have to assume some effective permittivity also. We compared the observed and calculated echo powers with changing effective permittivity assumption, and determined the most plausible effective permittivity.

Results: By applying the analysis method mentioned above, we could obtain the observed and calculated off-nadir surface echo powers. Based on them, we could estimate the effective permittivity of the lunar surface materials. The estimated effective permittivity is 2 - 3 in the highland, 3 - 4 in the maria. In addition, it was found that there areas whose effective permittivity reaching ~5 in the eastern part of Oceanus Procellarum and the western part of Mare Imbrium.

Discussion: By using the estimated effective permittivity of the lunar surface, we can derive the bulk density of the lunar surface materials. The derived bulk density is 1.2 - 1.8 g/cm³ in the highlands, 1.8 - 2.3 g/cm³ in the maria, and approximately 2.6 g/cm³ in the high-permittivity areas in Oceanus Procellarum and Mare Imbrium. The differences of estimated bulk density among the previous studies [Wieczorek et al., 2013; Carrier et al., 1991] and this study could be explained by the depth dependence of the bulk density of the lunar surface soils and rocks. The areas of high permittivity in the eastern part of Oceanus Procellarum and western part of Mare Imbrium coincide with young lava flow units in PKT region. We can consider two possible reasons: (i) The regolith layer is thinner than other mare regions due to short exposure to the meteorite impacts. (ii) The bulk density is higher than other mare regions due to high abundance of the ilmenite.

Keywords: SELENE(Kaguya), Lunar Radar Sounder (LRS), permittivity, Oceanus Procellarum, Mare Imbrium, Digital terrain model (DTM)

Relationship between topography and latest mare volcanism at 2.0 Ga of the moon

KATO, Shinsuke^{1*} ; MOROTA, Tomokatsu¹ ; WATANABE, Sei-ichiro¹ ; YAMAGUCHI, Yasushi¹ ;
OTAKE, Hisashi² ; OHTAKE, Makiko²

¹Division of Earth and Planetary Sciences, Graduate School of Science, Nagoya University, ²Japan Aerospace Exploration Agency

Lunar mare basalts, the most common volcanic feature on the Moon, provide insights into compositions and thermal history of lunar mantle. According to the radiometric ages of the lunar basalt samples and the model ages of mare basalt units determined by crater counting with remote sensing data, the great extent of mare basalts was formed at 3.2 to 3.8 Ga. Temporal variation of the mare basalt eruptions also indicates that magma activity has a second peak at the end of mare volcanism (~ 2 Ga), and the latest eruptions were limited in the Procellarum KREEP Terrane (PKT), which is characterized by high abundances of heat-producing elements. In order to understand the magma source of the latest volcanism and mechanism for causing the second peak, we examined the correlation between the titanium contents and eruption ages of mare basalt units using compositional and chronological data updated by SELENE/Kaguya. Although the systematic relationship is not observed globally, a rapid increase in mean titanium (Ti) content occurred at 2.3 Ga in the PKT, suggesting that the magma source of mare basalts changed at that time. The high-Ti basaltic eruptions can be correlated with the second peak of volcanic activity at ~ 2 Ga. The latest volcanic activity can be induced by a high-Ti super hot plume originated from the core-mantle boundary. If the super hot plume was occurred, the topographic features formed by the super hot plume may be remained. Then, we calculated the difference between topography and selenoid and found the circular feature like a plateau in the center of the PKT, which scale is ~ 1000 km horizontal and ~ 500 m vertical. Moreover, mare ridges in this region seem to connect with the plateau. Using detailed models of the flexural response of the lunar elastic lithosphere, we estimated the elastic thickness at the time of occurrence of the super hot plume. From our results, the effective elastic thickness at the period of latest volcanism is estimated 20 – 30 km, which is thinner than that of the period before ~ 2 Ga. These results suggest that the up lift of lithosphere caused by the super hot plume.

Keywords: titanium content, super hot plume, selenoid, effective elastic thickness, lunar mantle, the Procellarum KREEP Terrane

Impact history in the last 3 billion years based on the lunar rayed craters

KATO, Mami^{1*} ; MOROTA, Tomokatu¹

¹Nagoya University Graduate School of Environmental Studies

The Moon preserves the impact history in the last 4.0 Ga as the cratering record, which provide important information to understand collisional and orbital evolutions of small bodies in the solar system. Standard lunar cratering chronologies have been based on combining radiometric ages of Apollo and Luna samples and crater densities of landing sites. However, the impact history cannot be resolved in the past 3.0 Ga because of the absence of samples with radiometric age ranging from 3.0 to 1.0 b.y. On the other hand, from crater density of lunar rayed craters and statistics of terrestrial craters it has been suggested hypotheses that the cratering rate has increased or decreased in recent.

In this study, we determined relative ages of rayed craters using SELENE/TC image data to place constraints on the cratering rate in the last ~ 1 Ga. Formation age of the surface of the planet can be estimated by crater counting, based on the idea that old area have more craters than young area. We performed crater counting on the ejecta blanket of 67 rayed craters larger than 20 km in diameter. The results indicate that 27 rayed craters are younger than the crater Copernicus, whose the formation age is estimated as 0.81 Ga from the Apollo 12 samples.

Based on the crater density of rayed craters younger than Copernicus, the average cratering rate for craters larger than 10 km in diameter in the past 0.81 Ga is estimated to be $5.56 \times 10^{-4} \text{ km}^{-2} \text{ y}^{-1}$, which is 0.66 times lower than that in the past 3.2 Ga. The main source of impactors in the Earth-Moon system is the main asteroid belt located between the orbits of the Mars and Jupiter. The decreasing cratering rate revealed in this study indicates that the total number of asteroids in the main belt has been decreasing for last 3.0 Ga.

Keywords: Moon, crater, cratering chronology

Lunar surface areas with featureless reflectance spectra revealed by hyperspectral remote sensing

YAMAMOTO, Satoru^{1*}; NAKAMURA, Ryosuke²; MATSUNAGA, Tsuneo¹; OGAWA, Yoshiko³; ISHIHARA, Yoshiaki⁴; MOROTA, Tomokatsu⁵; HIRATA, Naru³; OHTAKE, Makiko⁴; HIROI, Takahiro⁶; YOKOTA, Yasuhiro¹; HARUYAMA, Junichi⁴

¹NIES, ²AIST, ³Univ. of Aizu, ⁴JAXA, ⁵Nagoya Univ., ⁶Brown Univ.

Spectral Profiler (SP) onboard SELENE/Kaguya has obtained continuous spectral reflectance data (hyperspectral data) for about 70 million points (0.5 by 0.5 km footprint) on the Moon in the visible and near-infrared wavelength ranges. Using a data mining approach with all the SP data (SP data mining), we have revealed the global distributions of several-kilometer-wide sites with exposed end members of various minerals on the lunar surface: olivine-rich sites, purest anorthosite (PAN) sites, orthopyroxene-rich sites, clinopyroxene-rich sites, and spinel-rich sites. These results are based on the analysis for the diagnostic absorption bands of $\lambda = 1\mu\text{m}$ and $2\mu\text{m}$ in the continuous reflectance data for the lunar major minerals. On the other hand, it has also been reported that there are several sites on the Moon exhibiting no absorption band for $1\mu\text{m}$ and $2\mu\text{m}$ (hereafter, featureless spectra or FL-spectra). However, it still remains unclear what is the origin for the FL spectra on the Moon. For the interpretations of the origin of the FL spectra, we need to understand the global occurrence trends of FL sites on the Moon. In this study, we conducted the global survey to reveal the global distribution of the FL sites using the SP data mining. From the global distribution data, we will discuss the possible mechanisms and its implications for the lunar primordial crust.

Keywords: remote sensing, hyperspectral, Moon, Kaguya/SELENE

Mineralogy of the lunar highland crust based on the Kaguya reflectance spectra

OHTAKE, Makiko^{1*} ; YAMAMOTO, Satoru² ; MATSUNAGA, Tsuneo² ; OGAWA, Yoshiko³

¹Japan Aero space Exploration Agency, ²National Institute for Environmental Studies, ³The University of Aizu

Introduction: The composition of the lunar highland crust is among the most important information for understanding the formation mechanism of the lunar highland crust and the composition of the lunar magma ocean. Previously, the composition of the lunar highland crust was estimated mainly based on measurements of the lunar returned samples. Measurements of returned lunar samples and meteorites indicate that the lunar highland crust typically consists of plagioclase and low-Ca pyroxene with minor amounts of other mineral phases. However, it is not clear if the low-Ca pyroxene really is a major mafic silicate component of the highland crust because the returned samples may not be a representative material of the entire highland crust. Therefore, this study investigated the mafic silicate phase and estimated its composition within the highland crust by using remote sensing reflectance spectra of the lunar surface.

Method: We used reflectance spectra acquired by the Kaguya Spectral Profiler (SP), which has a spectral coverage of 500 to 2600 nm in 300 bands and a spatial resolution of 500 x 500 m. Among the global SP data, all of the 570 purest anorthosite (PAN) [1] spectra identified and reported by [2] were analyzed by using the modified Gaussian model (MGM) [3]. Several MGM parameters, a number of fitted peak and peak parameters (center wavelength, width, and strength) of each peak at the starting point were tried, and the results were cross evaluated. The compositions of silicate mafic minerals were estimated by comparing the peak fit results and the known correlation between absorption center wavelength and mineral composition.

Results: Most (93%) of peak, which corresponds to the mafic silicate phase, has a center wavelength shorter than 980 nm, suggesting that these mafic silicates in the PAN rocks are low-Ca pyroxene (65% are shorter than 950 nm). Note that the low-Ca pyroxene in this study implies pyroxene having less than a 0.2 molar ratio of Ca/(Ca+Mg+Fe) smaller than 0.2. Data points having a center wavelength shorter than 980 nm had a strong absorption band and were not a product of weak ambiguous absorption spectra. Six percent of the data have center wavelengths between 980 nm and 1040 nm, which correspond to the high-Ca pyroxene composition. The remaining 1% of the data with longer center wavelengths around 1050 nm possibly corresponds to olivine or glass. No apparent phase difference (low-Ca and high-Ca pyroxene difference) is observed between the nearside and the farside.

Discussion: Our results indicate that the majority of the PAN layer in the lunar highland crust globally consists of anorthite and small amounts of low-Ca pyroxene, the major mafic silicate component, rather than high-Ca pyroxene or olivine. This result is consistent with the previous work based on measurements of the lunar material from the lunar surface mixing layer with limited global coverage and confirms the homogeneous modal abundance within the lunar highland crust. The short center wavelengths of the PAN rocks at Jackson crater, which located at the farside highland suggest relatively higher Mg# (Mg/(Mg + Fe) in mole per cent) (around 70) in this region than the near side. This evidence is in good agreement with previous work [4], which suggests the presence of magnesian anorthosite in the farside highland.

References: [1] Ohtake, M. et al. (2009) *Nature*, 461, 236-240. [2] Yamamoto, S. et al. (2012) *Geophys. Res. Lett.*, 39, L13201. [3] Sunshine, J. et al. (1990) *J. Geophys. Res.* 95, 6955-6966. [4] Ohtake, M. et al. (2012) *Nature GeoSci.* 5, 384-388.

Keywords: Kaguya, Moon, crust, reflectance spectra

Unsupervised Classification of the Moon's Surface Reflectance Spectra and Geological Significance (1)

ISHIHARA, Yoshiaki^{1*} ; HAREYAMA, Makoto² ; OHTAKE, Makiko¹

¹JAXA, ²St. Marianna Univ. of Med.

Great successes of recent lunar missions provide vast amount of varieties of remote sensing data. Analysis of those new data provide some new key evidences, such as pure-plagioclase rocks (e.g., Ohtake et al., 2009) and olivine rich rocks (e.g., Yamamoto et al., 2010), for studying solidification process of the Lunar Magma Ocean (LMO) and following lunar evolutions. Those key evidences require us to reconsider the LMO solidification process. One approach to study this problem is requiring following step, reconstruction of compositions and structures for primitive crust by removing influences of volcanisms, impact cratering, and other geological effects. For reconstructing primitive crust, we have to generate a global geological map covers recent findings, so we started a project to build a new lunar geological map to reconstruct structures and composition of the lunar primitive crust. Because of huge volume of recent data set, fully manual classify by expert researchers is not realistic, and then, we have been trying to use some data mining methods for basic unit candidate estimation.

In this study, we show some classification results of SELENE Multiband Imager (MI) data and Spectral Profiler (SP) data applied data mining methods, and compare them with a fully manual classification result for a limited area. Our classification procedure consists of two steps; Independent Component Analysis (ICA) and Iterative Self-Organizing Data Analysis (ISO-DATA). Detail strategy of our procedure is presented by Hareyama et al. in this meeting.

Our procedure generally works well. The classification results in mare region indicate that could detect some types of mare basalt flows. Especially high-Ti basalt in Oceanus Procellarum and the Mare Tranquillitatis are clearly identified. Ejecta deposits of fresh ray craters are also clearly identified. In addition, we compare classification results our procedure around the Aristarchus region with that of fully manual classification result by a researcher (M.O.). These two agrees each other generally. Then, we consider our procedure capture the lunar geological context and useful for the first step of building lunar geological map.

Keywords: Moon, Geological Map, Unsupervised Classification

Study of carbon-bearing materials formed by impact process on the Moon

MIURA, Yasunori^{1*}

¹Visiting Univ.(In & Out)

Introduction:

In the solar system (terrestrial planets), it is required to study overall processes of volatile carbon between planets (with and without global air and water) and the Moon without global air. Recently author has studied such complicated and unsolved problems [1-4]. In the present paper, the collision formation of carbon-containing materials is mainly to discuss it on celestial bodies without global air (the moon, asteroids and Mercury) that do not have the atmosphere, especially on the moon [3].

Volatiles in the Moon :

The Moon has original reservoirs of carbon-bearing volatiles from successive growth of fine dust particles to become celestial body size. However, the Moon is close to planet Mars size, but the volatiles- reservoirs are difficult to keep during characteristic abrupt collision process to be escaped away[1-3].

Problem of carbon dioxides atmosphere :

Water vapor changes liquid phase by quenching process. However, carbon dioxides-rich atmosphere keeps in a gaseous state by relative cooling, so that it should be taken into something to hot air estimated from the experimental results. In this sense, Mars and Venus with carbon dioxides-rich atmosphere are difficult to form global water system if a global water should be present before global gas-rich system[3]. The Moon is therefore celestial body to discuss the interior carbon-bearing volatiles [3].

Formation of carbon-containing materials of the Moon:

Because the Moon has no atmosphere globally, two-stages growth of separated carbon-rich macro-grains with high-pressure form cannot be expected because of no collision with global air on the airless Moon [3]. It is only possible to grow macroscopically in the shallow interiors (from dust-growth or fragments of air planet separated) by successive meteoritic collisions on the surface[4]. Carbon-bearing materials on the Moon are localized and minor contents of carbon-bearing materials in the glass, carbon, carbide and carbonates related with shock-wave processes[1-3].

Problem of global water on the Moon:

It might discuss possible formation of global air and water on the Moon and celestial bodies from experimental results. From laboratory experiments, carbon-bearing air which might be possible to generate a global water on air- planets of Mars and Venus is generally difficult, but it is not impossible by the proposed two methods ideally. On the other hand, formation of global water on air-less Moon (also Mercury and asteroids) is relatively very difficult, but it might be not impossible if the Moon becomes global air-bearing celestial body prepared by any proposed process[3].

Summary:

- 1) Formation of the atmosphere and seawater to any celestial body such as the Moon, can be discussed from experimental results of carbon-containing materials formed.
- 2) Carbon dioxides atmosphere can be reduced or cooled from state-condition of hot gas by any proposed experiments.
- 3) Lunar carbon-bearing grains of glass, carbon, carbide and carbonate can be grown microscopically and locally in the interior by successive process of impacts.

Reference:[1] Miura Y. (2011): LPSC 42(2011), #2817.

[2] Miura Y. et. al. (1996) Antarctic Meteorites XX1(Tokyo), 107-110.

[3] Miura Y. (2015): LPSC2016 (LPI), #1811, #1666.

[4] Miura Y. (2009): Patent application.

Keywords: The Moon, Carbon-bearing materials, Impacts, Volatiles, Experiment, Global air and water

Solar wind-regolith interaction in space: Observations at Moon and Phobos

FUTAANA, Yoshifumi^{1*}

¹Swedish Institute of Space Physics

In this presentation, we discuss whether the backscattering of plasma particles is a common physical process of plasma-surface interaction in space. The backscattered protons were first discovered by a plasma package, MAP/PACE, on board the Japanese lunar orbiter, Kaguya. Later, the backscattered protons and neutral hydrogen atoms have been frequently reported near the Moon, for example, by the SARA sensor on Chandrayaan-1. We first review the characteristics of the backscattered protons observed in the lunar environment.

Then, we report the survey of the dataset from the ion sensor (IMA) on board Mars Express recorded during its close encounters to Phobos. During one of the closest encounters (~60 km) we could clearly identify proton signal apart from the solar wind. Careful assessment has lead us to conclude that the signal is the Phobos origin. The characteristics of the Phobos protons are quite similar to those of the reflected lunar protons. The observation provides the first evidence proving that the backscattering is a common process for regolith-plasma interaction in space.

Keywords: solar wind, proton reflection, regolith, Moon, Phobos, backscattering

Exploration of the lunar internal structure using a small-sized penetrator and its perspective

YAMADA, Ryuhei^{1*}; ISHIHARA, Yoshiaki²; KOBAYASHI, Naoki²; MURAKAMI, Hideki³; GOTO, Ken²; SHIRAISHI, Hiroaki²; TANAKA, Satoshi²; HAYAKAWA, Masahiko²

¹National Astronomical Observatory of Japan / RISE Project, ²Japan Aerospace Exploration Agency, ³Kochi University

Information about the lunar interior has been obtained by the seismic exploration through the Apollo mission, the gravimetric explorations of the Kaguya and GRAIL missions, and other geodetic observations such as the Lunar Laser Ranging (LLR). However, we have not sufficiently constrained the lunar deep mantle and the core from available geophysical data, and the material and temperature in the lunar deep region are still uncertain. In addition, we have some uncertainties even about lunar crustal thickness and structure. Clear detections of lunar seismic phases which pass through the lunar deep and crustal regions will be required to reveal the structures. The penetrator, a hard-landing probe with a high sensitive seismometer developed in the former LUNAR-A project, is a powerful tool to carry out new lunar seismic observation.

To demonstrate utility of the penetrator system for scientific observations, we proposed a mission plan, named APPROACH, in which one penetrator is loaded onto a small satellite launched by the 3rd Epsilon Launch Vehicle. In this proposal, we had some plans to perform scientific observations; those are determination of the lunar crustal thickness using travel time data from meteoroid impact events located by the ground observation of the impact flashes, current lunar seismic activities compared with that during the Apollo-era and the first heat flow measurement on the lunar highland. However, the proposal could not be accepted because the success rate of the observation with only one penetrator was insufficient for acceptance.

In this situation, we currently make a modification to the mission plan so as to load two small-sized penetrators onto the small satellite. We aim to reduce the size of the penetrator to two-thirds size keeping the already established high shock durability. In this presentation, we firstly report some plans to reduce size of the penetrator and the effect of the downsizing on scientific observations. Then, we describe scientific expectation from the seismic and heat-flow observation using the small-sized penetrator. Finally, we will discuss future plans to study the lunar origin and evolution by the lunar seismic observations using the penetrator system after the achievement of first observation by the system.

Keywords: Penetrator, Lunar internal exploration, Moonquake observation, Heat flow observation, Small-sized exploration satellite

Present status of the active X-ray spectrometer development for future lunar landing mission

NAGAOKA, Hiroshi^{1*} ; HASEBE, Nobuyuki¹ ; KUSANO, Hiroki¹ ; NAITO, Masayuki¹ ; SHIBAMURA, Eido¹ ; AMANO, Yoshiharu¹ ; OHTA, Tohru¹ ; FAGAN, Timothy¹

¹Waseda University

The Active X-ray Spectrometer (AXS) consisting of an active X-ray generator and a silicon drift detector (SDD) has been developed for future lunar landing missions. The AXS can determine the elemental composition of rock samples by X-Ray Fluorescence spectroscopy which provides the geochemical data of rock samples. The AXS has each outstanding features as excellent energy resolution, compact and light weight, low power consumption, and no high voltage power supply and no radioisotopes. The X-ray generator is made of some pyroelectric crystals, peltier device and thin metal target. The instrument of the AXS and the present status of its development are presented and discussed.

Keywords: X-ray fluorescence spectroscopy, active X-ray spectrometer, lunar landing mission, elemental analysis

Study on X-ray Fluorescence for Future Lunar Landing Mission - Surface Roughness and Ratios of Characteristic X-ray -

NAITO, Masayuki^{1*} ; HASEBE, Nobuyuki¹ ; NAGAOKA, Hiroshi¹ ; KUSANO, Hiroki¹ ; KUWAKO, Masaki¹ ; OYAMA, Yuki¹ ; SHIBAMURA, Eido¹ ; AMANO, Yoshiharu¹ ; OHTA, Toru¹ ; MATIAS LOPES, Jose A.²

¹Waseda University, ²University of Coimbra

Landing and roving observation for planetary bodies provides more detailed local information of geochemistry, mineralogy and petrology with remote sensing observation[1]. An X-Ray Fluorescence spectroscopy (XRF) is a powerful method on/around the landing point in-situ measurement of chemical abundance. Lunar surface is so heavily weathered by meteorites, micrometeorites, the solar wind, and the cosmic rays that surface grindings of lunar samples should be performed by a rock abrasion tool to remove the weathered surface before the XRF measurements. The relations between surface roughness of sample and ratios of observed characteristic X-ray intensity are studied on the basis of both experiments and simulations[2, 3]. In this presentation, the results of experiments and simulations of grinding level needed for the XRF measurements on planetary surface are compared and discussed.

[1] T. Hashimoto et al., 2011, Acta Astronautica 68, 1386-1391. [2] H. Kusano et al., 2013, Proc. SPIE 8852, 88520B. [3] M. Naito et al., Nucl. Instrum. Methods Phys. A, to be published.

Keywords: Lunar sample, X-ray fluorescence, Active X-ray Spectrometer, Surface roughness

Visual Tracking using SIFT to Solve Time-Delay Problem in Remote Operation

NISHIYAMA, Hiroyuki^{1*} ; SHIMIZU, Sota² ; NAGAOKA, Hiroshi¹ ; HASEBE, Nobuyuki²

¹Dept. of Applied Physics, Waseda University, ²ARISE, Waseda University

This paper proposes and describes a method to solve a time-delay problem when a direction of a camera in the wide angle fovea vision system (WAFVS) equipped on a lunar exploring rover is controlled remotely from the ground control station on the earth. That is, we need to control the camera view direction accurately in order to obtain visible ray band images of a target in detail using WAFVS, but the time-delay often causes WAFVS to fail to capture the target in the central field of view of the input image when the rover is moving around. The authors achieve correct camera view direction control by applying SIFT operator to track a target candidate from past images to future images stored temporarily in the computer on the rover. Experimental results show this implementation is successfully done and indicate how to apply WAFVS for this task.

Keywords: Exploring Rover, Remote Operation, Visual Tracking, SIFT, Wide Angle Fovea Sensor, Time Delay

Toward a 3D spherical modeling of lunar mantle convection

OGAWA, Masaki^{1*} ; YANAGISAWA, Takatoshi² ; KAMEYAMA, Masanori³

¹Graduate School of Arts and Sciences, Univ. of Tokyo, ²Japan Agency for Marine-Earth Science and Technology, ³Geodynamic Research Center, Univ. of Ehime

Earlier two-dimensional models of coupled magmatism-mantle convection system raise two issues concerning the evolution of the lunar mantle. One is to understand why lunar magmatism continuously occurs with a characteristic time of several hundred million years. When the Rayleigh number of the lunar mantle Ra exceeds the critical value for the onset of thermal convection R_c , earlier two-dimensional models suggest that a positive feedback, called the magmatism-mantle upwelling (MMU) feedback, operates to make magmatism episodic and vigorous; magmatism occurs continuously and mildly as observed on the Moon only when $Ra < R_c$. Another issue is to understand why mare magmatism continued until as recent as about a billion years ago. Magmatism extracts heat producing elements (HPEs) and earlier two-dimensional models predicts that lunar magmatism should have waned much earlier because of this HPEs extraction. A possible solution to this issue is that the lunar mantle contains a reservoir that is enriched in HPEs and compositionally dense at depth. The nature of thermal convection in a basally heated mantle with a small core, however, has not been investigated enough to resolve these issues. To estimate R_c and to understand the nature of thermal convection in the lunar mantle, we are carrying out a linear perturbation analyses and numerical simulation of thermal convection in a spherical shell with a small core.

Keywords: the Moon, mantle evolution, 3D spherical shell, mantle convection, numerical simulation

Flow patterns in spherical mantles with small size of core; the effect of temperature dependent viscosity

YANAGISAWA, Takatoshi^{1*} ; OGAWA, Masaki² ; KAMEYAMA, Masanori³

¹Japan Agency for Marine-Earth Science and Technology, ²Graduate School of Arts and Sciences, Univ. of Tokyo, ³Geodynamic Research Center, Univ. of Ehime

Clarifying the effects of three-dimensional spherical geometry on mantle convection is a major issue of mantle dynamics in terrestrial planets. We study in detail the nature of thermal convection of a variable viscosity fluid in the basally heated spherical mantle of small planets with a small core, keeping in mind the application of our numerical models to the Moon. Spherical geometry affects mantle convection mildly when the ratio of the core-radius to the planetary radius r_{CMB} takes an Earth-like value of 0.55, while it is thought to affect strongly when r_{CMB} is small like Moon around 0.2. Here, we investigate the flow pattern systematically for r_{CMB} from 0.1 to 0.6 with small to large viscosity dependence on temperature. We first estimate the critical Rayleigh number Rc for the onset of convective motion at various r_{CMB} and the magnitude of temperature-dependence of viscosity by a linear perturbation analysis. Then, we study the convective flow pattern of thermal convection above Rc by numerical simulation. The result of our simulation is in good agreement with the linear analysis. The nature of convective flow pattern considerably changes as r_{CMB} smaller than about 0.4. The flow pattern has smaller number of up- and down-wellings. We established regime diagrams of convection pattern in relation to the Rayleigh number and the temperature dependence of viscosity, for various value of r_{CMB} . Stronger temperature dependence of viscosity is necessary for realizing the stagnant-lid regime of convection for smaller r_{CMB} . It is due to the relatively smaller volume of high temperature region near the CMB. The horizontally averaged temperature at mid mantle remains low despite the strong temperature variation of viscosity when r_{CMB} is small.

Keywords: Moon, 3D spherical shell, mantle convection, size of the core, flow pattern

Formation of anorthosite on the Moon through magma ocean fractional crystallization

ARAI, Tatsuyuki^{1*} ; TSUCHIYA, Taku² ; MARUYAMA, Shigenori³

¹Department of Earth and Planetary Sciences, Tokyo Institute of Technology, ²Geodynamics Research Center, Ehime University, ³Earth-Life Science Institute, Tokyo Institute of Technology

Geological records of the moon have a potential to reveal early evolution of the earth. 4.4Ga anorthosite on the Moon formed as by fractional crystallization of the lunar magma ocean (LMO). It has been generally accepted that the lunar bulk composition is enriched in FeO compared with the bulk silicate earth, which is critical to make large plagioclase/melt density difference enough to form the anorthosite. However, the bulk moon composition likely has the same composition of the earth, which is supported by isotopic similarities for the two bodies and recent giant impact modeling. In this study, critical condition of fractional crystallization of plagioclase is assessed for the BSE composition by taking into account crystal/melt density difference, viscosity of melt, crystal size, and Rayleigh number of the magma ocean. This study modeled solidification process of the LMO and calculated change of melt composition by use of MELTS/pMELTS. Density and viscosity of melt were calculated by use of first-principles simulations.

Results of thermodynamic calculations indicate that melt is basaltic (Mg# = 0.59) when plagioclase starts to crystallize. Viscosity of the basaltic melt ranges 20 - 10 Pa s whereas density ranges 2.60 - 2.71 g/cc for 0 - 1 GPa where plagioclase crystallizes. Comparison between critical crystal diameter calculated from the viscosity and density and crystal diameter of plagioclase (5 - 18mm) of anorthosite suggests that crystal fraction of magma, $\varphi = 0.55$ is required to make convection of magma ocean moderate enough that plagioclase could separate from the melt. Results of critical crystal diameter for olivine/pyroxene indicate that the crystallized mafic minerals would also be entrained in the viscous basaltic melt until $\varphi = 0.55$ is attained. In that case, large amount of mafic minerals are entrained in the magma along with plagioclase, which is enough to account for the $\varphi = 0.55$ in the magma. For the melt composition when crystal fraction $\varphi = 0.55$ is attained, the basaltic melt is enriched in FeO enough that plagioclase could float to the surface of the moon. Application of the discussion to the terrestrial magma ocean has insight into the surface evolution of the Hadean Earth, which would be related to the evolution of life.

Keywords: Moon, Anorthosite, Magma ocean, Density and viscosity of melt, Hadean Earth

High pressure phase relationships of the Fe-Ni-C system and its implications to the lunar core structure

KISHIMOTO, Shumpachi^{1*} ; URAKAWA, Satoru¹

¹Graduate school of natural science and technology, Okayama University

We investigate the phase relationships of the Fe-Ni-C systems at 5 GPa equivalent to the lunar core condition using multi anvil high pressure apparatus. We determined the precise melting relationships of the Fe-Ni-C system at 5 GPa. We also elucidate the stability field of (Fe,Ni)₃C and (Fe,Ni)₇C₃ carbide phase. In the meeting we will discuss the composition and the structure of the lunar core using the present data based on the seismic model of Weber et al. (2011).

Keywords: high pressure, lunar core, Fe-Ni-C system, phase relationships

Particle simulations on plasma and dust environment near lunar vertical holes

MIYAKE, Yohei^{1*} ; NISHINO, Masaki n²

¹Graduate School of System Informatics, Kobe University, ²The Solar-Terrestrial Environment Laboratory, Nagoya University

Japanese lunar explorer "Kaguya" has discovered vertical holes on the Moon surface. The diameter and depth of the holes are both in a range of 50 through 100 m, which produces a higher depth-to-diameter ratio than typical impact craters. The holes are thus expected to create characteristic plasma and dust environment around it. It is of practical importance to assess such a distinctive environment, reminding that a future landing mission plans to explore the lunar holes and caverns associating to the holes.

In the present study, we apply our original particle-in-cell simulator EMSES, which have been used to study spacecraft-plasma interactions, to assessment of day-side plasma environment around lunar vertical holes. We have a three-dimensional computational domain including a simplified lunar hole structure and introduce a solar wind plasma inflow to the lunar surface. We also simulate the photoelectron emission from the lunar surface by taking into account the presence or absence of sunlight illumination, and its incident angle. We will show simulation results on the properties of lunar surface charging near the hole and its dependence on changing solar wind plasma conditions. We also report the progress of further investigations into dust grain environment around the hole, based on the electrostatic environment self-consistently computed by our simulator.

Keywords: Moon, vertical hole, space plasma, lunar surface charging, dust grain, PIC simulation

Full Particle-In-Cell 3D simulation on the solar wind response to a lunar magnetic anomaly

USUI, Hideyuki^{1*} ; UMEZAWA, Misako¹ ; MIYAKE, Yohei¹ ; NISHINO, Masakiⁿ² ; ASHIDA, Yasumasa³

¹Graduate school of system informatics, ²STELAB Nagoya University, ³RISH Kyoto University

The objectives of the current research is to reveal the plasma environment disturbed by the magnetic anomaly found on the moon surface by considering the plasma kinetics. In this study, by performing three-dimensional full Particle-In-Cell simulations, we will discuss the plasma response to Reiner Gamma which is one of the typical and famous magnetic anomalies on the moon. The size of a magnetic anomaly is characterized by distance L from its center at which the equilibrium is satisfied between the pressure of the magnetic field of the dipole and that of the solar wind. In the Earth's magnetosphere, L implies the magnetopause location. We particularly focused on meso-scale magnetic dipoles in which L is smaller than the gyroradius of ions in the solar wind but larger than the electron Larmor radius. Contrary to the Earth's magnetosphere, difference of dynamics between ions and electrons with respect to the local magnetic field play an important role in the magnetosphere formation. In other words, electron-ion coupling through a dipole field becomes important. The simulation results show that a meso-scale magnetosphere is clearly created even if the ion gyroradius is larger than L . We found that electron dynamics are important in the process of meso-scale magnetosphere formation. Around the distance of L from the dipole center, charge separation occurs because of the difference of dynamics between electrons and ions. Then intense electrostatic field is locally induced and ions, which are assumed unmagnetized in the meso-scale magnetic dipole, are eventually influenced by this electric field. We also examined the plasma dynamics at dayside magnetosphere. Ions which encounter the magnetic anomaly start to gyrate around the local magnetic field. However, electrons which are basically magnetized make drift motion with $E \times B$ velocity. This difference of the plasma dynamics causes intense boundary current in the dayside region. In the case of Reiner Gamma, the magnetic field is almost perpendicular to the solar wind. In such a situation, increase of plasma and magnetic field densities is found in the dayside region in the simulation results. We are also interested in the plasma response when the direction of IMF changes because the magnetic field reconnection occurring in the dayside region will affect the formation of the meso-scale magnetosphere. One of the interesting findings is that the solar wind ions do not reach the moon surface in Reiner Gamma. We will discuss this point by considering the plasma dynamics as well as the electrostatic field observed over the Reiner Gamma region.

Keywords: Magnetic anomaly, Reiner Gamma, Meso-scale magnetic dipole, Solar wind response, Plasma particle simulation

Ion cyclotron waves observed by Kaguya/LMAG around the moon in the Earth's magnetosphere

NAKAGAWA, Tomoko^{1*}; TSUNAKAWA, Hideo²

¹Information and Communication Engineering, Tohoku Institute of Technology, ²Department of Earth and Planetary Sciences, Tokyo Institute of Technology

Narrowband ion cyclotron waves as found by Apollo 15 and 14 Lunar Surface Magnetometers were detected in the magnetic field data obtained by MAP/LMAG magnetometer on board Kaguya at an altitude of 100 km above the moon in the tail lobe of the Earth's magnetosphere. The frequency of the waves was near the local proton cyclotron frequency. They had a significant compressional component. They were detected on the dayside, on the nightside, or above the terminator of the moon. Analysis of the waves detected by Kaguya would contribute the understanding of the moon-plasma interaction.

Keywords: ion cyclotron wave, Kaguya, LMAG, moon, cyclotron frequency, lobe

Observation of the solar wind protons and alpha particles over lunar magnetic anomalies

KATO, Daiba^{1*} ; SAITO, Yoshifumi² ; NISHINO, Masaki³ ; YOKOTA, Shoichiro² ; TSUNAKAWA, Hideo⁴

¹Department of Earth and Planetary Science, The University of Tokyo, ²Institute of Space and Astronautical Science, Japan Aerospace Exploration Agency, ³Solar-Terrestrial Environment Laboratory, Nagoya University, ⁴Department of Earth and Planetary Sciences, Tokyo Institute of Technology

Lunar surface is directly affected by solar wind because the Moon has neither thick atmosphere nor global magnetic field. However, there exist locally magnetized regions called lunar magnetic anomalies on the lunar surface. Strong lunar magnetic anomalies can prevent solar wind from impacting the lunar surface. Research on the interaction between solar wind and lunar magnetic anomalies has been carried out by in-situ observations, numerical simulations and laboratory experiments, since the discovery of the lunar magnetic anomalies in 1960s. Since lunar magnetic anomalies greatly affect the incident solar wind plasma and plasma around the Moon, investigation on the interaction between solar wind and lunar magnetic anomalies is quite important.

The solar wind consists of protons as a major component and several percent of alpha particles as a second major component.

The flux of the magnetically reflected solar wind ions is about several tens percent of the incident solar wind ion flux. So far, nobody has ever investigated the reflected solar wind ions over lunar magnetic anomalies in terms of the ion species. Since more than 90% of the solar wind ions are protons, the current knowledge of the interaction between solar wind ions and lunar magnetic anomalies is highly dependent on the behavior of protons. Note that the incident solar wind alpha particles can be detected clearly, but the reflected alpha particles are not easily observed. Thus analysis of both proton and alpha particles will led us to more detailed understanding of the plasma structure over lunar magnetic anomalies.

In this study, we have analyzed mass identified low energy ion data observed by a low energy ion mass spectrometer MAP-PACE-IMA on Kaguya. We have newly found that reflected protons and reflected alpha particles show significantly different behaviors over lunar magnetic anomalies. In most cases, the bulk velocity of the reflected ions is slightly reduced from the incident solar wind bulk velocity, and the temperature of the reflected ions is higher than the incident solar wind ions. We have found that the bulk velocity of the reflected alpha particles is much lower than the bulk velocity of the reflected protons. We have also found that the ratio of the reflected alpha particle flux to the incident solar wind alpha particle flux is much less than the ratio of the reflected proton flux to the incident solar wind proton flux. There seems to be multiple reasons why the existence of the reflected alpha particles were not clear; 1) there exists large difference in E/q (E : kinetic energy, q : charge) between incident solar wind alpha particles and the reflected alpha particles and 2) the reflected alpha particle flux is quite low. It clearly shows that the reflection of the solar wind ions is not an ideal magnetic mirror reflection but the reflection includes non-adiabatic processes.

Keywords: Moon, plasma, solar wind, magnetic anomaly

Early global expansion of the Moon: constraints from topographic characteristics on linear gravity anomalies

SAWADA, Natsuki^{1*} ; MOROTA, Tomokatsu¹ ; KATO, Shinsuke¹ ; ISHIHARA, Yoshiaki² ;
HIRAMATSU, Yoshihiro³

¹Nagoya University Graduate School of Environmental studies, ²Japan Aerospace Exploration Agency, ³Kanazawa University Graduate School of Natural Science and Technology

According to numerical models of the lunar thermal evolution, the lunar radius temporarily increased at the lunar early stage because of a thermal expansion resulted from mantle remelting after the magma ocean solidification. However, no clear evidence of lunar early global expansion was observed because many impacts have transformed the lunar surface. Recently, the Gravity Recovery and Interior Laboratory (GRAIL), which was launched in 2011 by NASA, measured the lunar gravity field with high accuracy. Andrew-Hanna et al. [2013] identified large linear gravity anomalies (LGAs) from the analysis of the GRAIL gravity data, and suggested that the LGAs resulted from ancient intrusions or dykes formed by magmatism with the global expansion. To test the hypothesis, we investigated topographical profiles across the LGAs. In addition, we determined formation ages of LGAs to constrain the timing of the global expansion.

We used 1/1024-degree gridded lunar topographic data from LOLA Data Archive [<http://imbrium.mit.edu/LOLA.html> LOLA_GDR(LRO L-LOLA-4-GDR-V1.0)]. The topographic profiles across the LGAs were calculated in a range of 300 km from the LGAs. We found graben-like topography along the LGAs, suggesting that the LGAs were formed in the tensile stress field accompanied with the global expansion.

We performed crater counting in areas of 50 km distance from the LGAs to constrain the timing of the global expansion. The estimated formation ages of LGAs are distributed in a range from 4.3 to 3.9 Ga with a peak at 4.1 Ga, corresponding to the oldest ages of the Apollo basaltic samples and lunar basalt meteorites [e.g., Terada et al., 2007]. The results suggest that the lunar global expansion began at 4.3 Ga.

We estimated the lunar radius change as a function of time based on the estimated ages. We assumed that the topography of the LGAs simply were a dale consisting of two normal faults. The increase of lunar radius is estimated to be ~2.2 km at most, consistent with the estimation from a lunar thermal model [e.g., Zhang et al., 2014].

Keywords: linear gravity anomaly, early global expansion, tensile stress, topography, crater chronology

Magnetic anomalies, dynamo and true polar wander of the Moon

TAKAHASHI, Futoshi^{1*}; TSUNAKAWA, Hideo²; SHIMIZU, Hisayoshi³; SHIBUYA, Hidetoshi⁴; MATSUSHIMA, Masaki²

¹Department of Earth and Planetary Sciences, Kyushu University, ²Department of Earth and Planetary Sciences, Tokyo Institute of Technology, ³Earthquake Research Institute, University of Tokyo, ⁴Department of Earth and Environmental Sciences, Kumamoto University

Applying the latest advanced paleomagnetic technique to the Apollo samples, it is now well established that the Moon once had an ancient core dynamo operated from 4.2 to 3.56 billion years ago, or even younger age. Because these results are based on paleointensity retrieved from unoriented samples, any directional information cannot be obtained. Instead, we focus on the magnetic anomalies on the Moon. Since the magnetization of the lunar crust in the magnetic anomalies could be records of an early core dynamo of the Moon, the magnetic anomalies may yield directional information of the lunar paleomagnetic field. Here we present results of our global survey of magnetic anomalies on the lunar surface using magnetometer data acquired by the Lunar Prospector and Kaguya spacecraft. Using an iterative inversion method, we extract magnetization vectors from well-isolated magnetic anomalies and derive the positions of paleomagnetic poles. We find two distinct clusters of the resultant paleomagnetic poles: one near the present rotation axis and the other at mid-latitude (Takahashi et al., 2014). The result is consistent with a dipole-dominated lunar magnetic field generated by a core dynamo that was reversing the polarity. It is also implied that the Moon experienced a polar wander event. Additional inversion results for well-isolated central magnetic anomalies based on the surface vector mapping method (Tsunakawa et al., 2014) suggest existence of the third cluster of the lunar magnetic pole.

References

- Takahashi, F., H. Tsunakawa, H. Shimizu, H. Shibuya, and M. Matsushima (2014), Reorientation of the early lunar pole, *Nature Geosci.*, **7**, 409-412, doi:10.1038/ngeo2150.
- Tsunakawa, H., H. Shibuya, F. Takahashi, H. Shimizu, and M. Matsushima (2014), Regional mapping of the lunar magnetic anomalies at the surface: Method and its application to strong and weak magnetic anomaly regions, *Icarus*, **228**, 35-53, doi:10.1016/j.icarus.2013.09.026.

Keywords: magnetic anomaly, dynamo, core, polar wander

Mare basalt volcanism within the giant impact structure of the Moon

TAGUCHI, Masako^{1*} ; MOROTA, Tomokatsu¹ ; KATO, Shinsuke¹

¹Nagoya University Graduate School of Environmental studies

Toward an understanding of the evolution of the Earth and other terrestrial planets, it is important to study the thermal evolution of the Moon. Estimate of volumes and eruption ages of lava ponds is essential to construct the volcanic history of the Moon. Therefore, these estimates have been performed in the lunar maria, a lowland area covered with basalt.

The South Pole-Aitken (SPA) basin, located on southern lunar farside, is one of the oldest and largest impact structures in the solar system. The basin ranges ~13 km in depth, and its rim crest diameter is about 2500 km. Previous studies of numerical simulation for SPA-forming impact indicate that the large impact generated a melting zone ranging 500 km depth and changed the thermal condition of the underlying mantle.

In order to evaluate the effect of the SPA-forming impact on volcanic activity, we estimated the thickness and the volumes of lava ponds of Apollo, Leibnitz, Ingenii, located within the SPA, using high-resolution image data obtained by Kaguya. Volumes of these maria were estimated as 4440-7330 km³, 4880-12580 km³, and 5830-53570km³, slightly smaller than estimate of previous study. In comparing the volumes of lava ponds of northern lunar farside, there is no significant difference, suggesting that SPA-forming impact did not contribute to magma production.

Keywords: SPA, mare volcanism, Apollo, Leibnitz, Ingenii

Global spatial distribution of the lunar craters characterized by the Voronoi tessellation

ITO, Riho¹ ; HONDA, Chikatoshi^{1*} ; HIRATA, Naru¹ ; MOROTA, Tomokatsu²

¹The University of Aizu, ²Graduate School of Environmental Studies, Nagoya University

A surface of bodies in the solar system has been exposed by numerous numbers of impact craterings. The impact craters are formed by the hypervelocity impact of meteorites or interplanetary bodies. The impact craterings basically occur at random on the planetary surface. However, the surface of the Moon, which has same rotation and revolution periods, is expected to indicate a bias of spatial distribution of craters even though the surface has a same formation age. According to theoretical analyses, cratering rate altered by this synchronized rotation effect indicates maximum at the apex of leading side and minimum at the trailing side (Zahnle et al., 2001; Le Feuvre and Wieczorek, 2011). On the other hand, this asymmetry of crater spatial distribution by synchronized rotation effect was assessed by Morota et al. (2005) and Werner and Medvedev (2010). Morota et al. (2005) showed that number density of rayed craters at the apex is the highest on the lunar surface. Werner and Medvedev (2010) showed that peak of high number density of rayed craters observed at the distance of about 60° from the apex where is at the leading side including the apex. Because the formation term of rayed craters is in the past from the present to 1 Ga, the synchronized rotation effect of impact cratering had been achieved in this term.

A purpose of this research is to assess the spatial distribution of the global lunar craters without distinction of rayed or not. The assessed craters contain older craters than that of rayed craters, so we could evaluate the synchronized rotation effect at the ancient time before the rayed crater formation. By using the Voronoi tessellation, the global spatial distribution of the lunar craters have the potential of differences by assessing several crater-sets. A result of this research might suggest that the synchronized rotation effect to the lunar craters was not identified in the term before rayed crater formation. In addition to this result, we confirmed the effect of secondary craters which were produced by the Orientale basin formation near the apex.

Keywords: lunar craters, spatial distribution, Voronoi tessellation

Three-dimensional lunar mare subsurface structures based on the SELENE radar sounding

ISHIYAMA, Ken^{1*} ; KUMAMOTO, Atsushi¹ ; NAKAMURA, Norihiro²

¹Department of Geophysics, Tohoku University, ²Department of Earth Science, Tohoku University

In order to discuss the history of the lunar volcanic activity, the lunar geological maps have been produced on the basis of the surface crater age [e.g., Hiesinger et al., 2000], surface composition [e.g., Lucey et al., 2000], and terrain morphology [e.g., Haruyama et al., 2008] of the lava flow units in the mare region [e.g., Hiesinger et al., 2000; Hackwill et al., 2006; Bugiolacchi and Guest, 2008]. These maps lack subsurface information, although the lunar mare subsurface structure was obtained from the radar sounding of the Apollo 17 mission in 1972 and the SELENE (KAGUYA) mission during 2007-2008. Subsurface information provides useful data for discussing the continuity and discontinuity of the geological strata. Thus, we will verify the lunar geological interpretation based on the lunar surface information.

The Lunar Radar Sounder (LRS) onboard the SELENE spacecraft carried out the global exploration of lunar mare subsurface structures by radiating the electromagnetic wave (4-6 MHz) and detecting the reflectors from the surface and subsurface boundary [Ono et al., 2009]. Compared to the LRS data with the preexisting geological maps, previous studies have been discussed the eruption flux of the lava flow [Oshigami et al., 2014] and geological condition (i.e., porosity and density) of the mare region [Ishiyama et al., 2013]. In order to merge the subsurface information into the geological map, we investigated the depth of the subsurface reflectors at the interval of 1 deg. in latitude and $< \sim 2$ deg. in longitude and produced the three-dimensional database of the subsurface structures. In the presentation, we will show three-dimensional mare subsurface structures found in this study.

An interpretation of formation process of the lunar highland crust using Th distribution map and crustal thickness data

YAMAMOTO, Keiko^{1*} ; HARUYAMA, Junichi¹ ; KOBAYASHI, Shingo² ; OHTAKE, Makiko¹ ; IWATA, Takahiro¹ ; ISHIHARA, Yoshiaki¹

¹Japan Aerospace Exploration Agency, ²National Institute of Radiological Sciences

On the lunar highland area, correlation between spatial patterns of the surface Thorium abundance measured by SELENE gamma-ray spectrometer and the crustal thickness from GRAIL gravity field and LRO topography was investigated. Although several local minima areas exist in Thorium abundance map, each of these minima is not as significant as the others. On the other hand, in crustal thickness map, one of the areas has significantly large magnitude compared to others. To explain the discrepancy, we propose a two-stage process scenario of the crustal formation, i.e., formation of plural thin plateaux on the surface of the Moon, which correspond to the observed surface Thorium distribution, and following development to enlarge lunar dichotomic feature by downward growth of the plateaux. Our interpretation for the discrepancy is consistent with the previously proposed crustal formation scenarios that the dichotomy was developed during the crustal formation process.

Keywords: Thorium abundance, lunar crustal thickness, SELENE, GRAIL, lunar crustal formation

Mineral distribution on lunar highland in the southwest sector of the Crisium basin with SELENE MI

SUGAMIYA, Takeshi^{1*} ; HIRATA, Naru¹

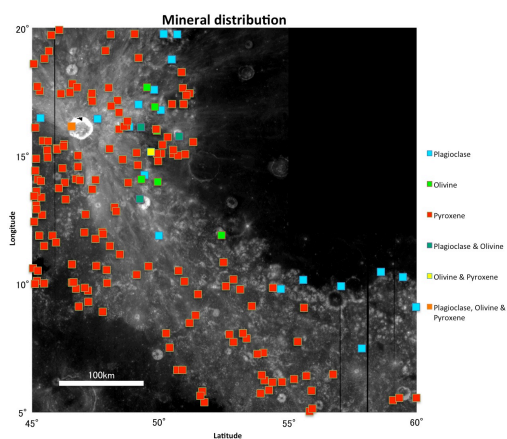
¹CAIST/ARC-Space, The University of Aizu

SELENE (Kaguya) Multiband Imager (MI) provides a global and homogeneous spatial coverage of multiband data set of the moon. Its spectral coverage ranges visible and near infrared wavelength including absorption features of major lunar highland minerals: plagioclase, olivine, and pyroxene. We perform an extensive survey of mineral outcrops with MI multiband data on lunar highland in the southwest sector of the Crisium basin. It is reported that outcrops of these major minerals are found in this region by sparse survey with SELENE (Kaguya) Spectral Profiler observation (Nakamura et al., 2012; Yamamoto et al., 2010, 2012, 2014). It is also expected that a large impact event forming the Crisium basin excavate vertical stratigraphy of lunar highland, and possibly mantle materials.

Possible mineral outcrops are identified at which deep absorptions are found in continuum-removed spectra of MI. Position of absorption centers of plagioclase, olivine, and pyroxene are 1250, 1050, and 950 nm, respectively. Most outcrops are associated to craters in the target regions. They are often found on the inner wall and the ejecta blanket of craters.

Plagioclase outcrops exhibit PAN (purest-anorthosite) like spectra with the clear 1250 nm absorption that was reported by Ohtake et al. (2009) and Yamamoto et al. (2012). Most of them are found at small craters with diameter of <1 km, whereas Ohtake et al. (2009) reported that PAN were found mainly on craters with diameter of >30 km. However, our researched region is placed adjacent or within the Crisium basin. As Yamamoto et al. (2012) suggested, PAN blocks could be excavated from deep region of the highland crust by the Crisium basin impact event. We also confirm an observation by Yamamoto et al. (2012) that olivine outcrops also associate with PAN exposures in this region.

Keywords: SELENE, MI, the Moon, Highland, Plagioclase, Mare Crisium



Unsupervised Classification of the Moon's Surface Reflectance Spectra and Geological Significance (2)

HAREYAMA, Makoto^{1*} ; ISHIHARA, Yoshiaki² ; OHTAKE, Makiko²

¹St. Marianna University School of Medicine, ²Japan Aerospace Exploration Agency

Clarifying of lunar geological map is essential in understanding the initial formation of lunar crust and the mixing process of lunar surface rocks due to igneous activities and meteorite impacts. However, the global geological map shown today has been published in the 1980s after the Apollo era, which does not include various new knowledge found in recent exploration. Therefore, we started a project to make a new global geological map of the Moon based on new data as topography, mineral and elemental composition acquired by Japanese lunar explorer "Kaguya".

A basic item for the project is a classification map of reflectance spectra obtained by Multiband Imager (MI) and Spectral Profiler (SP) aboard Kaguya, which include information of rock and mineral kinds. However, since the data collected by MI and SP is very huge, data processing for whole moon is impossible to complete by working of only human's eyes and hands. And, the classification should be exclude researcher's subjective or philosophy as possible, especially in the first phase of analysis. Standing this point of view, we adopt ISODATA (Iterative Self-Organizing Data Analysis Technique) method as Unsupervised Classification (UC) with Independent Component Analysis (ICA) for classification of the reflectance spectra.

ICA is a powerful tool for analysis of multispectral or hyperspectral datasets to extract mutually independent components (ICs) from a set of mixed-random signals. This work is the first examination to apply ICA to the reflectance spectra from lunar surface, though ICA has been adopted to lunar gamma-ray spectra obtained gamma-ray spectrometer onboard Kaguya [10]. It was found that the global maps of extracted ICs clearly showed some mineral and/or rocks distributions as true signals, some characteristic patterns as noises due to mechanical and observational conditions and many random noises.

After ICA, the signal ICs are put in UC. This work employed ISODATA method as UC. ISODATA calculates class means evenly distributed in the data space then iteratively clusters the remaining pixels using minimum distance techniques. Users do not need to know the number of clusters and can define threshold values for parameters as minimum distance or minimum number of pixels for a class and so on. As a result, whole moon were divided into 50 -100 classes, though it was depended on the threshold values.

This report will shows the detail procedure for classification of lunar reflectance spectra and discusses validity and applicability of this procedure based on the results.

Keywords: Moon, Geological Classification, Reflectance, Independent Component Analysis, Unsupervised Classification, Kaguya

Gravity anomaly uncorrelated with topography in the Moon and its origin

UCHIDA, Mako^{1*} ; ISHIHARA, Yoshiaki² ; HIRAMATSU, Yoshihiro¹

¹Kanazawa Univ., ²JAXA

Based on the gravity field model with the spherical harmonics up to degree and order 420 estimated from the observation data of the initial mission phase of GRAIL, Zuber et al. (2013) reported that, from order and degree of 80 to 300, 98% of the gravity disturbance potential of the Moon is caused by the topography and the remaining 2% of it is uncorrelated with the topography but is caused by subsurface high-density materials. Recent analysis of GRAIL data of the all mission phases provides the gravity field model with the spherical harmonics up to degree and order 900 (Lemoine et al. 2014; Konopliv et al., 2014). We can, therefore, expect to obtain detailed information of the interior of the Moon from this model. In this study, from the latest selenodetic data, we detect areas where gravity anomaly is uncorrelated with lunar topography, estimate the density structure of the crust beneath the areas, and infer its origin.

We use the topographic model of LRO_LTM01_PA_1080 with the spherical harmonics of degree and order 1080 (Neumann, 2013). Bouguer anomaly is calculated from the topographic data and the gravity potential data of GRGM900C (Lemoine et al., 2014) with the Bouguer correction density of 2560 kg/m³ and is expanded by the spherical harmonics of degree and order 600 based on the accuracy of the gravity data (Lemoine et al., 2014). We estimate the depth of the lunar Moho using a gravity inversion of Wieczorek and Phillips (1998) and subtract the Bouguer anomaly caused by the relief of the Moho from the original one. This Bouguer anomaly, hereafter referred to as the residual Bouguer anomaly, represents gravity anomaly caused by density anomalies in the crust. In the estimation of the Moho depth, we set the crustal density of 2750 kg/m³ and the mantle density of 3360 kg/m³ so that our estimation coincides with seismological estimations of the crustal thickness at Apollo 12/14 sites and the average crustal thickness reported by previous works. We detect 23 areas where the residual Bouguer anomaly is uncorrelated with the topography. For 14 areas where distinct positive anomaly is recognized, we estimate the shape and the position of a high-density body (a density contrast of 610 kg/m³) in the crust using the prism approximation of Banerjee and Gupta (1977). The other 9 areas are characterized by nearly zero residual Bouguer anomaly, suggesting that the relief of the Moho causes the gravity anomaly uncorrelated with the topography.

The estimations for all 14 areas show that the shape of the high-density body is sill-like and the body is located at the base of the crust, in other words adjacent to the Moho. Comparing the reflectivity map of the wavelength of 750 nm produced by the multi-band imager of the SELENE (Ohtake et al., 2008) to the location of the 14 areas, we reveal that the 14 areas are distributed in the lunar mare with low reflectivity. The 14 areas are distributed along ridges and/or rings of impact basins. These facts suggest that the high-density bodies are related to past igneous activity and the formation process of the ridges and impact basins.

From the above, we propose a following scenario. The formation of cracks in the crust accompanied with the formation of the ridges and impact basins promotes the magma intrusion into the crust. Insufficient pressure and buoyancy due to poor volatiles makes the magma intrude laterally like sill at the base of the crust near the Moho. We suggest that high-density bodies with long wavelength are modeled as the relief of the lunar Moho because the density of the bodies is considered to be comparable to the mantle density.

Acknowledgements: We use the topographic data released by the LOLA Data Archive (<http://imbrium.mit.edu/LOLA.html>) and the gravity data released by the NASA PDS Geoscience Node (<http://pds-geosciences.wustl.edu/missions/grail/default.htm>). We also use the SHTOOLS (<http://shertools.ipgp.fr>) for the calculations in this study.

Keywords: ridge, impact basin, gravity inversion, intrusion, magmatism

The effect of thermal fatigue on the moon surface

ANDO, Kosuke^{1*} ; MOROTA, Tomokatsu¹

¹Graduate School of Environmental Studies, Nagoya University

The surface condition of the Moon and asteroids reflects its geological evolution. In fact, the surface conditions are very different between celestial bodies. For example, the Moon is almost covered with fine regolith layer, on the other hand, boulders and regolith cover an asteroid Itokawa.

As usual, it has been thought that the collision of micro bodies was dominant as for the origin of regolith. However, recently, it is pointed the possibility that thermal fatigue is more dominant than collision on asteroids (Delbo et al., 2014). In this study, we investigate the size distribution of boulders around small craters at equator and high latitude, and discuss the effect of thermal fatigue on grain refining of boulders. In this study, we used the high-resolution images obtained by LRO.

The result shows that the size distributions of boulders around and in small craters differ with craters, reflecting the ages of small craters. Fresher craters have large boulders, and older craters have less large ones because boulders are destroyed with time. We will discuss the latitude dependence of the boulder destruction rate.

Water trapped at lunar regolith

HASUNAKA, Ryota^{1*}

¹Department of Earth and Space Science, Graduate School of Science, Osaka University

We simulated the behavior of water in lunar regolith, and examined if water could be trapped for a long term. The situation for our simulation corresponds to the lunar surface shined by the Sun at noon, whereas the situation at permanently shaded areas is simulated by Schorghofer¹ and Taylor (2007). Transportations of heat and water vapor could be expressed by similar-form equations, namely the diffusion equations. We observed condensation of ice at the deep part of the regolith, at latitudes higher than 84°. Our results indicate that water could be trapped at >10 cm depth layer of the lunar regolith. The trapped water could correspond to the "hidden" water resource at lunar surface, which is not visible by remote-sensing observation.

Keywords: moon, regolith, water, simulation

Features of 3D shapes of lunar regolith particles: comparison with Itokawa particles and experimental impact fragments

SAKURAMA, Takashi^{1*}; TSUCHIYAMA, Akira¹; NAKANO, Tsukasa²; UESUGI, Kentaro³

¹Division of Earth and Planetary Sciences, Graduate School of Science, Kyoto University, ²Geological Survey of Japan, AIST, ³SPRING-8/JASRI

To understand formation and evolution of regolith on airless bodies such as the moon and asteroids, 3D shape distributions of regolith particles have been measured and compared with those of experimental high-speed impact fragments. The 3D shapes of asteroid Itokawa particles recovered by the Hayabusa spacecraft were measured using X-ray microtomography [1], and it was proposed that the 3D shape distributions of Itokawa particles are undistinguishable from those of experimental impact fragments [2], but lunar particles from Descartes Highlands (Apollo 16 sample; 60501) [3] are more spherical than Itokawa particles. Lunar particles from Mare Tranquillitatis (Apollo 11 sample; 10084) are also more spherical than Itokawa particles [4]. However, as these returned samples were imaged grain by grain, the data collection was time-consuming, and thus the numbers of particles measured were limited up to about sixty. In addition, it is necessary to obtain more data efficiently for lunar samples, which may have variety. In this study, more lunar regolith samples were efficiently examined by tomography to understand 3D shape features of lunar regolith particles and compare those with Itokawa particles and experimental impact fragments.

In the present study, in addition to the Apollo samples (10084 and 60501), we used Luna samples; L1613-3 (Luna 16: Mare Fecunditatis), L2001-4 (Luna 20: Apollonius Highlands) and L24130.3-2,3,4 (Luna 24: Mare Crisium). The sample particles were attached on a toothpick with double-sided tape to take CT images at once by X-ray microtomography. Imaging experiments were made at BL20B2 of SPRING-8 with the X-ray energies of 17.9, 18.1 or 20 keV and voxel size of 1.73 μm . Particles were extracted by binarization. The isolated particles having more than 10,000 voxels, which are possible for significant 3D shape measurement [5], were analyzed. So far, we have examined 156 and 90 particles of 10084 and L2001-4, respectively.

The axial lengths of particles were measured by ovoid approximation (OA) and bounding box (BB) method [4]. In BB method, the axial lengths differ if the order of determination of the shortest, intermediate and longest lengths (S, I and L, respectively) is different. We adopted two methods, where S was determined first followed by I and L corresponding to the impact fragments of [6] and L was determined first followed by I and S corresponding to [2]. The axial ratios, I/L and S/I, were plotted as Zingg diagrams. These 3D shape distributions were compared with the previous data of lunar regolith particles [3,4], Itokawa particles [7] and experimental impact fragments [2,5,6] using Kolmogorov-Smirnov (K-S) test.

There is no significant difference between the particle shape distributions of the same sample with different imaging methods (grain by grain or many particles at once) at least for 10084. As far as the samples analyzed and the previous samples concerned, there are basically no significant differences of the shape distributions among lunar samples irrespective of mare and highland samples. In contrast, the lunar particles are more spherical than the Itokawa particles and the experimental impact fragments. Because residence time scale of particles in lunar regolith is long (the order of one billion years) [8], it is possible for lunar regolith particles to become spherical by abrasion due to gardening. We are planning to report the results of more samples in the presentation.

[1] Tsuchiyama et al. (2011) *Science* 333: 1125. [2] Capaccioni et al. (1984) *Nature* 308: 832. [3] Katagiri et al. (2014) *J. Aerosp. Eng.* 10: 1061. [4] Tsuchiyama et al., (2013) *Goldschmidt Conf. Abstract* 2361. [5] Shimada (2014) Masters thesis (Graduate School of Science, Osaka University). [6] Fujiwara et al. (1978) *Nature*, 272: 602. [7] Tsuchiyama et al (2014) *MAPS*, 49: 172. [8] Wieler (2002) *Rev. Mineral. Geochem.*, 47: 21.

Keywords: Apollo mission, Luna mission, Hayabusa mission, X-ray tomography, SPRING-8

Development of hollow type retroreflector for future LLR - thermal tolerance test of the optical contact surface -

ARAKI, Hiroshi^{1*} ; KASHIMA, Shingo¹ ; NODA, Hirotomo¹ ; YASUDA, Susumu² ; UTSUNOMIYA, Shin² ; TSURUTA, Seiitsu¹ ; ASARI, Kazuyoshi¹ ; OTSUBO, Toshimichi³ ; KUNIMORI, Hiroo⁴

¹National Astronomical observatory of Japan, ²Japan Aerospace Exploration Agency, ³Hitotsubashi University, ⁴National Institute of Information and Communications Technology

The contribution of Lunar Laser Ranging (LLR) since its installation in 1969 is quite significant, for example, to the construction of lunar ephemeris and celestial reference frame, gravitational physics, Earth-Moon dynamics, and lunar interior structure. However, one order or more accurate ranging data than present level (2cm as normal point) are needed to enhance our understanding on the lunar deep structure. We are developing "single aperture and hollow" retroreflector (Corner Cube Mirror; CCM) having no optical pass difference for future lunar landing missions. Last year we presented CCM made of mono crystalline silicon shows the best performance through thermal and optical simulations in the lunar thermal environment. As for the fabrication method of CCM, we investigate mainly "three-plane bonding" with the optical contact technique, by which three plane mirrors are optically contacted on side with each other. It is known the shear strength of optically contacted surface increases as the annealing temperature becomes high. Quantitative data on this hardening effect are crucial for design and fabrication of CCM. We, therefore, have conducted high temperature exposing experiment of the optically contacted test pieces of mono crystalline silicon in the air from 100 °C to 1000 °C and confirmed that the shear strength along the thermally processed surface at 1000 °C becomes 5 or 6 times higher than original strength and the degradation of surface accuracy and roughness can be ignored. The 20cm aperture CCM model is under fabrication now. Results of accurate measurements of the dihedral angles of the CCM model by ZYGO interferometer will be presented to quantify the effect of the thermal annealing.

Keywords: LLR, CCM, hollow, optical contact, thermal, strength

SELENE-2/Lunar ElectroMagnetic Sounder (LEMS): a test of inversion (2)

MATSUSHIMA, Masaki^{1*} ; SHIMIZU, Hisayoshi² ; TOH, Hiroaki³ ; YOSHIMURA, Ryokei⁴ ;
TAKAHASHI, Futoshi⁵ ; TSUNAKAWA, Hideo¹ ; SHIBUYA, Hidetoshi⁶ ; MATSUOKA, Ayako⁷ ; ODA, Hirokuni⁸ ;
OGAWA, Kazunori⁹ ; TANAKA, Satoshi⁷

¹Tokyo Institute of Technology, ²ERI, University of Tokyo, ³Kyoto University, ⁴DPRI, Kyoto University, ⁵Kyushu University,
⁶Kumamoto University, ⁷ISAS/JAXA, ⁸AIST, ⁹University of Tokyo

The so-called giant impact hypothesis is likely to explain the origin of the Moon in view of physical and chemical evidence such as angular momentum, materials possibly through magma ocean processes, and compositional similarity of the Earth and the Moon. Numerical simulations of such a giant impact indicate that most of the Moon-forming material around the proto-Earth originates from the projectile. This means that such a standard giant impact is difficult to form the Moon whose isotopic composition is essentially identical to the Earth's as found from the lunar samples in the Apollo mission. This would be a reason why new giant-impact models are devised. It should be noted that the lunar samples were obtained only from the lunar surface, and that information on bulk composition and interior structure of the Moon is still insufficient. Therefore it is of significance to obtain information regarding the whole lunar composition and interior structure, which can advance our understanding of lunar origin and evolution.

In the SELENE-2 mission, we propose a lunar electromagnetic sounder (LEMS) to estimate the electrical conductivity structure of the Moon. The electrical conductivity varies with temperature even for the same composition, and therefore it can be used to deduce the present thermal structure of the Moon.

Temporal variations in the magnetic field of lunar external origin, which can be observed by magnetometers onboard a lunar orbiter and a lunar lander, induce eddy currents in the lunar interior depending on the electrical conductivity distribution and frequencies of the temporal variations. The eddy currents, in turn, generate temporal variations in the magnetic field of lunar internal origin, which can be observed by a magnetometer onboard a lunar lander. Thus electromagnetic response of the Moon is obtained by magnetic field measurements. Then the electromagnetic response function is used to estimate the electrical conductivity structure by solving an inverse problem. We show results for some tests of inversion, assuming a one-dimensional interior structure for electrical conductivity distribution.

Keywords: electromagnetic sounding, lunar interior structure, SELENE-2